Theoretical investigation of electronic structure, electric field gradients, and photoemission of $PuCoGa_5$ and $PuRhGa_5$ superconductors

Alexander B. Shick,[1] Ján Rusz,[1,2] Jindřich Kolorenč,[1,3] Peter M. Oppeneer,[2] and Ladislav Havela[4]
[1]*Institute of Physics, Academy of Sciences of the Czech Republic, Na Slovance 2, CZ-182 21 Prague, Czech Republic*
[2]*Department of Physics and Astronomy, Uppsala University, Box 516, S-751 20 Uppsala, Sweden*
[3]*University of Hamburg, Jungiusstraße 9, D-20355 Hamburg, Germany*
[4]*Department of Condensed Matter Physics, Charles University, Ke Karlovu 5, CZ-12116 Prague, Czech Republic*
(Received 5 August 2010; revised manuscript received 15 December 2010; published 5 April 2011)

We report electronic structure calculations of $PuCoGa_5$ and $PuRhGa_5$ superconductors. The band structure, electric field gradients, and Fermi surface topologies were investigated using two methods of correlated band theory, namely the conventional static mean-field LDA+U and the local density matrix approximation (LDMA). The latter is based on the Hubbard-I approximation and includes intra-atomic dynamical correlations in a self-consistent manner. Our results show that although LDA+U and LDMA calculations do not significantly modify the Fermi surface topologies compared to LDA, they do lead to a substantial reduction of the f character of the electronic states at the Fermi energy. The calculations indicate presence of a pseudogap in the electronic spectrum. We achieve a good agreement between calculated and experimental nuclear quadrupolar resonance frequencies and a fairly good agreement between calculated and experimental photoemission spectra. Our findings can be important for the theory of superconductivity in $PuCoGa_5$ and related compounds.

DOI: 10.1103/PhysRevB.83.155105 PACS number(s): 71.27.+a, 74.70.Tx, 76.60.Gv, 74.25.Jb

I. INTRODUCTION

The nature of mediating bosons responsible for electron pairing in the superconducting phase of $PuCoGa_5$ and related compounds remains controversial even after a decade long intense research that has followed the discovery of the superconducting transition in these materials.[1] The most frequently expressed view is that they are unconventional superconductors driven by spin fluctuations.[2] Nevertheless, polarized neutron scattering experiments[3] have shown that the normal state of $PuCoGa_5$ is different from the anticipated magnetic plutonium f^5 ion, since the observed magnetic susceptibility in the normal state is weak, temperature independent, and dominated by orbital effects. This fact may cast some doubts on the importance of the magnetic degrees of freedom for formation of the superconducting phase in this compound.

Various electronic structure calculations were performed to study the normal phase of the $PuCoGa_5$ and related compounds. The local density approximation (LDA) resulted in a large weight of the $5f$ states at the Fermi level, and suggested that the superconductivity in $PuCoGa_5$ dominantly emerges due to the $5f$ states of Pu.[4] Later on, static[5,6] (LDA+U) and dynamical[7] (LDA+FLEX) correlated band theory calculations confirmed the nonmagnetic and intermediate-valence character of plutonium atoms in $PuCoGa_5$ and $PuRhGa_5$.

In this work we study electron correlation effects in the electronic structure of these materials. We make use of the local density matrix approximation[8] (LDMA) to the dynamical mean-field theory that combines the Hubbard-I approximation (HIA) with the full-potential linearized augmented plane wave (FP-LAPW) method[10] and includes full self-consistency over the charge density. The LDMA results are compared with the outcome of conventional LDA+U calculations that utilize two different versions of the FP-LAPW: an in-house LDA+U implementation[11] as well as the WIEN2k package.[12] The latter incorporates evaluation of the electric field gradients[13] (EFG) using methods described in Refs. 14 and 15.

This paper is organized as follows. In Sec. II we recall the basic equations of the LDMA.[8] In Sec. III we present results obtained for $PuCoGa_5$ and $PuRhGa_5$. We start with summarizing the electronic structure and electric field gradients calculated with the LDA+U approximation. Next, we show the electronic structure, Fermi surfaces, and photoelectron spectra provided by the LDMA method. These results are compared with available experimental data. The relation between the electronic structure and superconducting properties is discussed.

II. COMPUTATIONAL METHOD

As we have shown before, the LDMA substantially alleviates the deficiencies of the conventional LDA+U method in the description of the electronic structure of elemental actinides (see Refs. 8 and 9 for a detailed comparison with experimental data and with other dynamical mean-field theory calculations).

In the LDMA, the local occupation matrix

$$n_{\gamma_1\gamma_2} = -\frac{1}{\pi}\,\mathrm{Im}\int_{-\infty}^{E_F} \mathrm{d}z\,[G(z)]_{\gamma_1\gamma_2} \tag{1}$$

represented in a basis $\{\phi_\gamma\}$ is self-consistently evaluated with the aid of the local Green's function $G(z)$,

$$[G(z)]^{-1}_{\gamma_1\gamma_2} = [G_{\mathrm{LDA}}(z)]^{-1}_{\gamma_1\gamma_2} - \Delta\epsilon\,\delta_{\gamma_1\gamma_2} - [\Sigma_{\mathrm{H}}(z)]_{\gamma_1\gamma_2}, \tag{2}$$

where $\Sigma_{\mathrm{H}}(z)$ is the HIA self-energy, $\Delta\epsilon$ accounts for the difference between the impurity and the lattice chemical potentials, and $G_{\mathrm{LDA}}(z)$ is the LDA Green's function,

$$[G_{\mathrm{LDA}}(z)]_{\gamma_1\gamma_2} = \frac{1}{V_{\mathrm{BZ}}}\int_{\mathrm{BZ}} \mathrm{d}^3k\,[z+\mu-H_{\mathrm{LDA}}(\mathbf{k})]^{-1}_{\gamma_1\gamma_2}. \tag{3}$$

The local density matrix $n_{\gamma_1\gamma_2}$ is used to construct an effective LDA+U potential

$$V_U = \sum_{\gamma_1\gamma_2} |\phi_{\gamma_1}\rangle \Bigg[\sum_{\gamma\gamma'} (\langle\gamma_2\gamma|V^{ee}|\gamma_1\gamma'\rangle - \langle\gamma_2\gamma|V^{ee}|\gamma'\gamma_1\rangle) n_{\gamma\gamma'} - V_{dc}\delta_{\gamma_1\gamma_2} \Bigg] \langle\phi_{\gamma_2}| \,, \quad (4)$$

where V^{ee} denotes the effective on-site Coulomb interaction and V_{dc} stands for the double-counting term. The potential V_U is inserted into Kohn-Sham–like equations,[16]

$$[-\nabla^2 + V_{\rm LDA}(\mathbf{r}) + V_U + \xi(\mathbf{l}\cdot\mathbf{s})]\Phi^b_{\mathbf{k}}(\mathbf{r}) = \epsilon^b_{\mathbf{k}}\Phi^b_{\mathbf{k}}(\mathbf{r}) \,, \quad (5)$$

that are iteratively solved until self-consistency over the charge density is reached. In the end, the eigenvalues and eigenvectors of Eq. (5) represent the correlated band structure and the imaginary part of the local Green's function $G(z)$, Eq. (2), provides a means to estimate valence-band photoemission spectra.

The LDMA extends the LDA+U approximation in several important aspects—it goes beyond the single Slater determinantal wave functions for the description of the intra-atomic processes and thus inherently incorporates intermediate coupling regime and accounts for multiplet transitions within the f shell.

III. RESULTS AND DISCUSSION

In all calculations we used the LDA optimized crystal structure parameters[4] of $PuCoGa_5$: lattice constant $a = 7.842$ a.u., ratio $c/a = 1.602$, and internal Ga-atom position $z = 0.304$ in the tetragonal $HoCoGa_5$ structure. In the FP-LAPW method we set the radii of the atomic spheres to 3.1 a.u. (Pu), 2.3 a.u. (Co), 2.4 a.u. (Rh), and 2.3 a.u. (Ga). The parameter $R \times K_{\rm max} = 10.2$ determined the basis set size and the Brillouin zone (BZ) sampling was performed with 1152 k points unless noted otherwise in the main text. For the plutonium f shell, Slater integrals $F_0 = 3.00$ eV, $F_2 = 6.53$ eV, $F_4 = 4.38$ eV, and $F_6 = 3.24$ eV were selected to specify the Coulomb interaction. They correspond to commonly accepted values for Coulomb $U = 3$ eV and exchange $J = 0.55$ eV parameters.

A. LDA+U calculations

Recently it was shown that LDA+U with the around-mean-field (AMF) double counting[17] applied to $PuCoGa_5$ and $PuRhGa_5$ compounds leads to a collapse of local magnetic moments (both spin and orbital part) on Pu atoms rendering the whole compound nonmagnetic.[6,7] This is in agreement with experimental studies[3] which for $PuCoGa_5$ report no detectable magnetic order down to 1 K and show only low induced magnetization in external magnetic fields. In this respect the situation is similar to δ-Pu where the same kind of calculations yields neither spin nor orbital magnetic moment,[5] along with solid experimental evidence for the lack of magnetic order.[18]

At first, we have confirmed the earlier results[6] for the nonmagnetic ground state in $PuCoGa_5$ employing WIEN2k package.[12] The calculated AMF-LDA+U band structure is shown in Fig. 1, where the character of the eigenstates

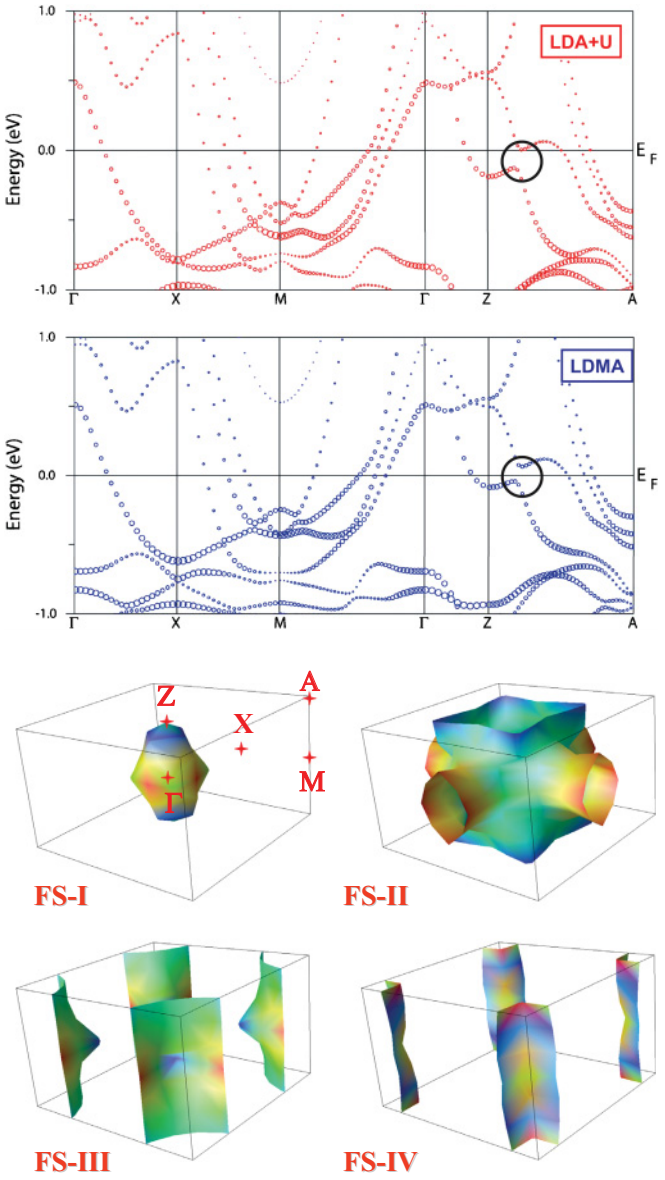

FIG. 1. (Color online) The LDA+U calculated band structure (top), the LDMA calculated band structure (middle), and LDMA Fermi surface (bottom) of $PuCoGa_5$ for $U = 3$ eV.

is indicated by circles whose size is proportional to the f-state spectral weight. Note that both employed FP-LAPW implementations are in a close agreement with each other. Comparison with the LDA band structure shown in Fig. 3 of Ref. 4 indicates that by increasing the value of U, the f bands move away from the Fermi level E_F. The occupied bands are affected relatively little by the on-site Coulomb U—they shift down by less than 1 eV for $U = 3$ eV—while the unoccupied $5f$ bands move up in energy much more steeply with increasing U. This general observation is also valid for the $PuRhGa_5$ compound.

Following the analysis of the band structure, we have used the WIEN2k code to calculate the electric field gradients in $PuCoGa_5$ and $PuRhGa_5$. Brillouin zone sampling with 2000 k points turned out to be sufficient to determine the EFG on Ga atoms with an accuracy better than 0.5%. A recent study of

the electronic structure and electric field gradients in related Ce-115 compounds demonstrated that the nuclear quadrupole resonance (NQR) is a sensitive probe of the local electronic structure.[19]

The electric field gradients V_{zz} are related to nuclear quadrupolar resonance frequencies ν_Q by a formula

$$\nu_Q = V_{zz}\frac{3eQ}{2I(2I-1)h}\sqrt{1+\frac{\eta^2}{3}}, \qquad (6)$$

where h is the Planck's constant, e is the electron charge, and η is a dimensionless asymmetry parameter. There are two stable isotopes of gallium, ^{69}Ga and ^{71}Ga, which have rather different nuclear quadrupolar moments Q of 0.171 b and 0.107 b,[23] whereas their nuclear spin I is the same, $I = 3/2$. The constant factor expressed as a fraction in Eq. (6) has values 2.067 MHz m^2 V^{-1} and 1.293 MHz m^2 V^{-1} for ^{69}Ga and ^{71}Ga, respectively.

In the tetragonal unit cell (P4/mmm structure) there are two different Ga sites: the Ga(1) (1c site) and Ga(2) (4i site). Ga(1) is located in the Pu–Ga plane and has axial symmetry and hence $\eta = 0$, whereas Ga(2) located between the Pu–Ga and Co or Rh planes has a lower symmetry and nonzero η. The calculated LDA+U results for two values of U, 0 and 3 eV, are summarized in Table I. The measured quadrupolar frequency of ^{69}Ga at the Ga(1) position in $PuRhGa_5$ (Ref. 22) is close to the value obtained by our LDA+U calculations with $U = 3$ eV. For the Ga(2) position there are reported values for both isotopes. The value of its asymmetry parameter η is again best reproduced by LDA+U calculations with $U = 3$ eV. If we use the calculated η, we obtain quadrupolar frequencies for the Ga(2) position given in Table I, which would indicate best agreement with experiment for calculations with $U = 0$ eV. Note, however, that the calculations with $U = 3$ eV are also very close to experimental values with only $\approx$3% error. Generally, compared to the Ga(1) site, the calculated NQR at the site Ga(2) is less sensitive to the value of U applied on the Pu site. A similar observation was made also in the case of Ce-115 compounds,[19] where the ν_Q at In(2) site depends only weakly on details of electronic structure at the Ce site. We can thus conclude that LDA+U calculations with $U = 3$ eV provide a consistent interpretation of the measured $PuRhGa_5$ NQR data.

TABLE I. Nuclear quadrupolar resonance frequencies ν_Q (MHz) and the dimensionless asymmetry parameter η at Ga(2). See text for discussion of $PuCoGa_5$ experiment.

	$U = 0$ eV	$U = 3$ eV	Exp.[20,22]
		ν_Q [MHz] at ^{69}Ga(1)	
$PuCoGa_5$	18.18	14.64	–
$PuRhGa_5$	16.40	13.01	13.22
		ν_Q [MHz] at ^{69}Ga(2)	
$PuCoGa_5$	27.26	26.31	28.28[21]
$PuRhGa_5$	29.33	28.48	29.15
		ν_Q [MHz] at ^{71}Ga(2)	
$PuCoGa_5$	17.05	16.46	17.69[21]
$PuRhGa_5$	18.35	17.81	18.38
		η at Ga(2)	
$PuCoGa_5$	0.290	0.319	0.20
$PuRhGa_5$	0.373	0.401	0.42

TABLE II. 5f-state occupations n_f, $n_f^{5/2}$, and $n_f^{7/2}$, and branching ratio B for $PuCoGa_5$. The atomic data are adopted from Ref. 24.

	n_f	$n_f^{5/2}$	$n_f^{7/2}$	B
LDMA	5.32	4.61	0.71	0.851
LDA+U	5.38	5.20	0.18	0.913
atomic IC	5	4.23	0.77	0.816
atomic IC	6	5.28	0.72	0.980
atomic jj	5	5.0	0.0	0.896
atomic jj	6	6.0	0.0	1.0

For $PuCoGa_5$ there are published NQR data in Ref. 20. We note however that the reported ^{69}Ga NQR values[20] were originally attributed to the Ga(1) position, but this response stemmed most likely from gallium atoms at the Ga(2) position.[21] This viewpoint is consistent with our theoretical predictions; the reported ν_Q value of 28.28 MHz would not correspond to the calculated ^{69}Ga(1) ν_Q values and neither to the Ga(1) ν_Q measured on isoelectronic $PuRhGa_5$ (Ref. 22). Our calculated values for the Ga(2) site in $PuCoGa_5$ are also close to the measured value, when this is attributed to Ga(2). Nonetheless, a re-evaluation of the NQR experimental data on $PuCoGa_5$ would be desirable to provide accurate NQR values.

B. LDMA calculations

In Table II we show LDMA and LDA+U results for the total f-shell occupation n_f, its decomposition into the occupations of $j = 5/2$ and $j = 7/2$ subshells, and the branching ratio[24] B for $PuCoGa_5$. Comparison is made with the results of intermediate-coupling (IC) and jj-coupling calculations performed for atomic f^5 and f^6 configurations.[24] It is apparent that the f shell in the solid is different from the isolated atomic f^5 shell, indicating an intermediate-valence state of the Pu atom in $PuCoGa_5$. This observation is in qualitative agreement with the experimental measurements of the neutron scattering form factor.[3]

The total occupations n_f resulting from LDA+U and LDMA calculations are similar. What differs are their subshell components $n_f^{5/2}$ and $n_f^{7/2}$, and the corresponding branching ratios. Like in the elemental actinides,[8,24,25] the LDMA produces an intermediate-coupling ground state, whereas the LDA+U solution is close to the jj limit. This disparity is a direct consequence of different Hilbert spaces used for the f shell in evaluation of the local occupation matrix $n_{\gamma,\gamma'}$: LDMA uses the complete many-body Hilbert space with dimension 2^{14} constructed on the top of the 14 local f orbitals, whereas LDA+U employs only the single-particle Hilbert space spanned on these orbitals.

C. Fermi surface topology and related properties

Analogously to the LDA+U, the LDMA eigenvalues and eigenvectors from Eq. (5) represent the correlated band structure. Examination of its plot in Fig. 1 shows that the f character in the vicinity of E_F is reduced in comparison with LDA.[4] This behavior is very similar to the LDA+U results discussed above.

The corresponding quasiparticle Fermi surfaces (FS) are also shown in Fig. 1. There are four sheets (I–IV) composing the FS: sheets I and II are fairly three-dimensional (3D) and sheets III and IV are two-dimensional (2D). Close similarities are revealed between these sheets and the Fermi surfaces from the previous LDA[4] and AMF-LDA+U calculations. Surprisingly, the Fermi surfaces calculated with LDMA and LDA have very similar geometry. This is particularly the case for the FS-III and FS-IV sheets, whereas there exist some differences for the FS-II sheet. Nonetheless, this implies that LDMA and LDA will give very similar results for the de Haas–van Alphen frequencies despite an important difference between LDMA and LDA: The f character at the Fermi surface is strongly reduced in LDMA compared to LDA.

Next, we calculate the band-resolved densities of states (DOS) for the bands forming the four Fermi surface sheets and the corresponding Fermi velocities defined as

$$|\langle v_i \rangle| = \sqrt{\frac{\int_{\mathrm{BZ}} \mathrm{d}^3k\, v_i^2 \delta(E(\mathbf{k}) - E_F)}{\int_{\mathrm{BZ}} \mathrm{d}^3k\, \delta(E(\mathbf{k}) - E_F)}}, \qquad (7)$$

where $v_i = \partial E(\mathbf{k})/\partial k_i$ is the group velocity along the ith direction ($i = x, y, z$). Calculated values of the DOS(E_F) and the Fermi velocities are shown in Table III. For all bands contributing to the Fermi surface, the value of fDOS(E_F) provides only a fraction of the total DOS(E_F). For FS-I and II we obtain a rather small anisotropy between the in-plane (x, y) and out-of-plane (z) velocities consistent with the 3D character of these sheets. For FS-III and IV, the values of the out-of-plane velocity are reduced due to the 2D character of FS-III and IV, and the in-plane values stay about the same as for FS-II as expected from the band structure shown in Fig. 1. Consequently, there is a noticeable anisotropy between the in-plane and out-of-plane velocities consistent with the 2D character of FS-III and IV. We note that quasi-2D character of the FS is also observed experimentally for materials from Ce115 family.[26]

The energy bands which correspond to the Fermi sheets I and II are apparently split by a gap along the **Z**–**A** direction (see Fig. 1). Further details can be found in Fig. 2 where we plot these bands in a plane cutting the Brillouin zone at $k_z = \pi/c$. The pseudogap (as it appears only in a part of the Brillouin zone) is visible along the **Z**–**R** line in this case. Figure 2 also shows a contribution to the density of states coming from the FS-I and FS-II bands. Two peaks in the DOS, one just below E_F for FS-I and the other just above E_F for FS-II are clearly visible. The occurrence of the pseudogap of approximately 0.15 eV separating the FS-I and FS-II bands correlates with these two peaks. The orbital character of the DOS indicated in Fig. 2 shows that most of the contribution to FS-I comes from Pu-f, Co-d, and Ga-p states, while FS-II consists mostly of Pu-f, Co-d, and interstitial states. None of these features are

TABLE III. The total and f-projected DOS(E_F) in eV^{-1}, out-of-plane and in-plane Fermi velocities in units of 10^5 m/s, and ratio of in-plane and out-of-plane upper critical fields for the four Fermi surface sheets from Fig. 1.

FS	DOS(E_F)	fDOS(E_F)	$\lvert\langle v_z\rangle\rvert$	$\lvert\langle v_{x,y}\rangle\rvert$	$H_{c2}^{a,b}/H_{c2}^{c}$
I	0.5	0.2	1.3	2.0	1.5
II	1.3	0.4	2.5	2.8	1.1
III	0.8	0.2	1.0	3.0	3.0
IV	0.5	0.1	0.9	3.0	3.3
Total	3.1	0.9	2.3	3.6	1.6

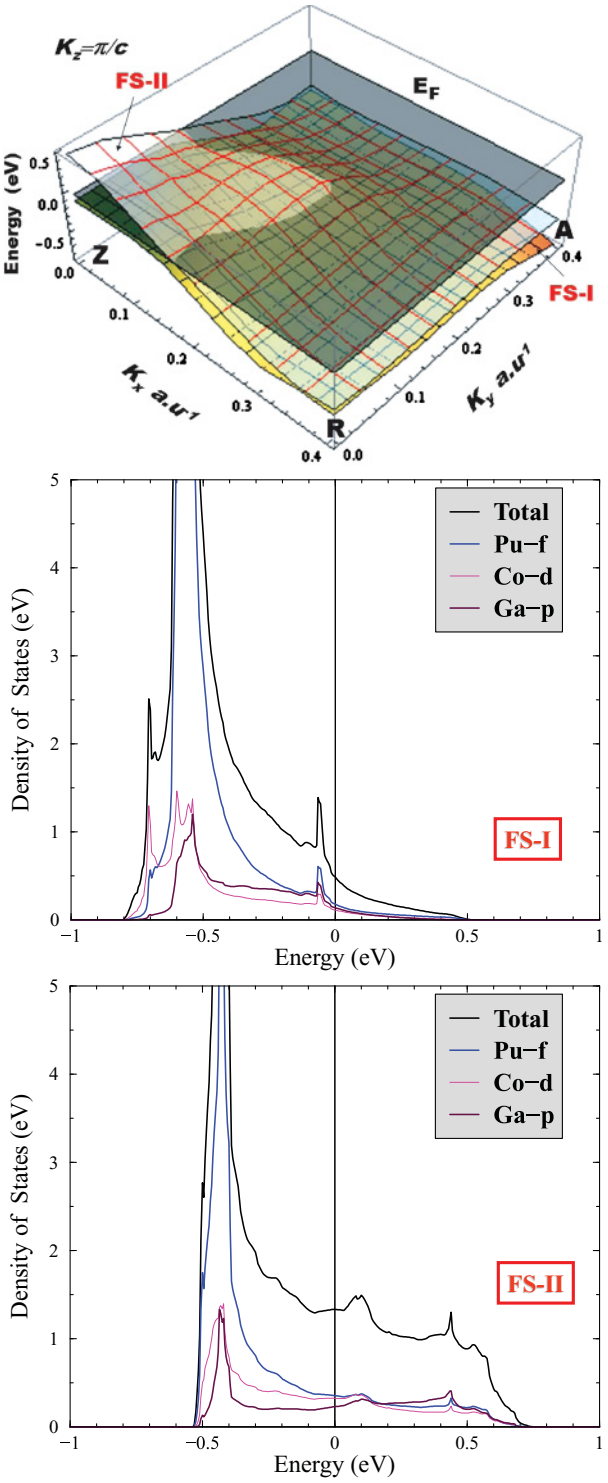

FIG. 2. (Color online) LDMA calculated energy bands of $PuCoGa_5$ corresponding to FS-I and FS-II plotted in a plane cutting the Brillouin zone at $k_z = \pi/c$. The Fermi energy plane is also shown (top); DOS for the FS-I and FS-II bands (bottom).

found for the bands that form the 2D-like Fermi sheets III and IV. The f character is further reduced in the FS-III and FS-IV bands with most of their spectral weight coming from Pu-f, Co-d as well as from interstitial states.

Very recently, a hybridization gap[27] in the DOS of $PuCoGa_5$ was observed in a pump-probe optical study.[28] The size of the gap was estimated about 4–5 meV, and its origin was attributed to the 2D-like Fermi surface sheets III and IV displaying dominant $5f$ character as obtained in the earlier LDA calculations.[4] Our results are qualitatively consistent with the presence of a (pseudo)gap in the spectrum and show that it is connected to the 3D-like components of the Fermi surface (FS-I and FS-II). The experiments[28] can hence be alternatively interpreted in terms of hybridization between f and non-f states near E_F, rather than in terms of delocalization of Pu $5f$ electrons.

D. Implications for superconductivity

Once the band velocities and the density of states at the Fermi level are known, the Drude plasma energy $\Omega_p = \sqrt{\frac{1}{3}\Omega_x^2 + \frac{1}{3}\Omega_y^2 + \frac{1}{3}\Omega_z^2}$ can be calculated. The individual directional components Ω_i are given as

$$\Omega_i^2 = \frac{e^2}{2\pi^2}\int_{\mathrm{BZ}} d^3k\, v_i^2 \delta[E(\mathbf{k}) - E_F], \tag{8}$$

which leads to numerical values $\Omega_x = \Omega_y = 4.2$ eV, $\Omega_z = 2.75$ eV, and $\Omega_p = 3.8$ eV. Using the Drude plasma energy, and assuming that the temperature dependence of electrical resistivity is only due to the electron-phonon interaction, we can estimate the electron-phonon coupling λ_{tr} from the Bloch-Grüneisen transport theory. At sufficiently high temperatures ($T \geqslant 0.7 \times \Theta_D$, i.e., above 170 K in the case of $PuCoGa_5$) we can employ an approximate expression[29]

$$\frac{\Delta\rho}{\Delta T} \approx \frac{8\pi^2}{\hbar\Omega_p^2} k_{\mathrm{B}}\lambda_{\mathrm{tr}} \tag{9}$$

which relates the electrical resistivity ρ and the electron-phonon coupling strength. Taking the experimental resistivity[32] at $T = 300$ K of $\approx 240\ \mu\Omega$ cm, and removing the residual value $\approx 30\ \mu\Omega$ cm, we get the remarkably large $\lambda_{\mathrm{tr}} = 2.5$.

First-principles LDA phonon calculations[30] give a substantially smaller value of $\lambda = 0.7$. Repeating the procedure outlined in the preceding paragraph for the LDA band structure[5] yields $\Omega_p = 2.2$ eV for the Drude plasma energy and $\lambda_{\mathrm{tr}} = 0.8$ for the electron-phonon coupling, which is quite close to $\lambda = 0.7$ derived from the LDA phonon calculations.[30] It illustrates the validity of Eq. (9) for semiquantitative estimate of the electron-phonon coupling strength. Apparently the LDMA λ_{tr} enhancement over its LDA value is due to an increase of the Drude plasma energy Ω_p, which in turn is caused by an increase of Fermi velocity, Eq. (7), when the Coulomb U is included. Generally, the electrons at E_F become faster as their f character is reduced.

To further assess the reliability of the LDMA and LDA estimates for the λ_{tr} parameter, we can turn to the comparison of experimental and calculated phonon spectra.[31] It was found that the conventional LDA/GGA band theory is not sufficient to accurately reproduce the lattice dynamics in $PuCoGa_5$. Better agreement with experimental data is achieved when Coulomb $U = 3$ eV (the same as used in our calculations) is included. It is therefore reasonable to assume that the larger electron-phonon coupling deduced from the LDMA electronic structure captures the reality better than the smaller LDA estimate.

Putting $\lambda_{\mathrm{tr}} = 2.5$ into the McMillan formula,[33] and assuming the Coulomb pseudopotential $\mu^* = 0.0$–0.2, we obtain an estimate for the superconducting transition temperature T_c in the range 27–39 K, which is not too far from the experimental value $T_c = 18.5$ K. This observation supports a strong electron-phonon coupling mechanism of superconductivity in $PuCoGa_5$ in line with the model recently proposed in Refs. 32 and 34.

Additional support for electron-phonon origin of superconductivity in $PuCoGa_5$ can be found in similarities with MgB_2 noticed already in the first LDA calculations.[4] Both compounds have Fermi surfaces composed of 2D and 3D sheets and the transition temperature appears to scale with the masses of the constituent atoms, namely $T_c^{\mathrm{MgB_2}}/T_c^{\mathrm{PuCoGa_5}} \approx \sqrt{M_{\mathrm{Ga}}/M_{\mathrm{B}}}$.

The electron-phonon interaction is always attractive. Conventional wisdom thus suggests that it would preferably lead to s-wave pairing. At first glance, it contradicts the results of Refs. 2 and 20 which show no evidence for a Hebel-Slichter coherence peak in the spin lattice relaxation rate ${T_1}^{-1}$ measurements. This absence points to unconventional, likely *d wave, superconductivity in PuCoGa*$_5$. It is often used as argument against electron-phonon interaction and in favor of an antiferromagnetic spin-fluctuation mediated pairing. Nevertheless, there are several scenarios where electron-phonon interaction induces unconventional superconductivity as well. Non-s-wave pairing can occur as a result of an interplay of spin and orbital fluctuations with electron-phonon interaction.[35] Alternatively, the s-wave channel in the electron-phonon mediated superconductivity can be suppressed by a strong on-site Coulomb interaction, which again leads to an unconventional pairing.[36] While we do not present here the microscopic mechanism for superconductivity in $PuCoGa_5$, we emphasize that the electron-phonon mechanism is not impossible.

As a next characteristic of the superconducting state we estimate the in-plane/out-of-plane anisotropy ratio for the upper critical field $H_{c2}^{a,b}/H_{c2}^{c}$ assuming that it is proportional to the ratio of the Fermi velocities $|\langle v_{x,y}\rangle|/|\langle v_z\rangle|$ (see Table III). There is almost no anisotropy in H_{c2} for Fermi sheets I and II, and a very pronounced anisotropy for sheets III and IV. Since very high magnetic fields are needed to reach H_{c2} in $PuCoGa_5$ at low temperatures, it is difficult to make a comparison with experiment. Recently, the upper critical field was carefully measured in $PuRhGa_5$, which displays lower H_{c2} values than $PuCoGa_5$.[37,38] Experimental anisotropy ratios of H_{c2} were found to fall in the range of 1.8 to 2.0 showing a reasonable agreement with our estimates.

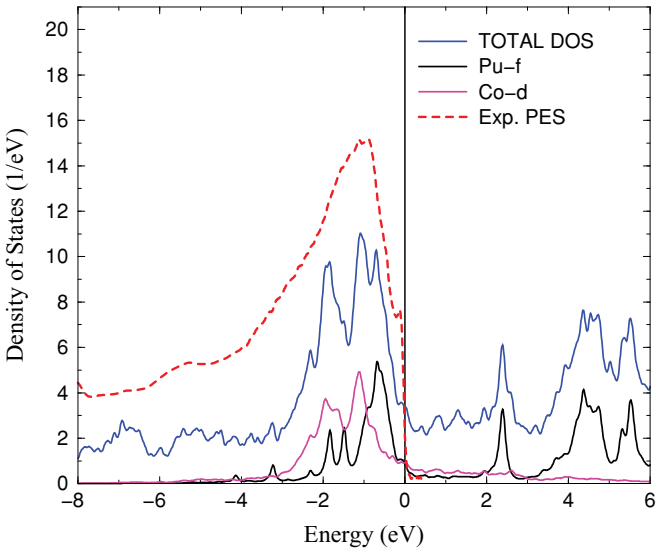

FIG. 3. (Color online) Spectral density (including multiplet transitions) of $PuCoGa_5$ provided by LDMA with $U = 3$ eV. Experimental PE spectrum (arb. units) from Ref. 40 is shown for comparison.

E. Valence-band photoemission

Valence-band photoemission (PE) data obtained with various photon energies[39] exhibit a relatively low f-state intensity at the Fermi level E_F, while most of the f-related emission is located in the energy range 0.5–3 eV below E_F. One representative PE spectrum is shown in Fig. 3. These data were obtained on sputter deposited films. They differ somewhat from the earlier PE results[40] that were obtained on a laser-ablated surface and display a weak but noticeable f peak near E_F. The occurrence of this sharp peak is consistent with predominantly f character of DOS at E_F seen in LDA calculations[4] and was used to argue in favor of the importance of f electrons for the emerging superconductivity. This feature close to the Fermi level remains visible in the results of Ref. 40 with substantially reduced intensity. Also the shape of the Pu-4f core level spectra, with weak intensity at the "well-screened" position, are compatible with a moderate f density of state at the Fermi level.[39]

The difference between the data of Refs. 40 and 41 can be due to a small excess of Ga at the surface of the samples used in Ref. 41. The Ga excess can be well monitored using ultraviolet photoelectron spectroscopy (UPS) of Ga-3d core-level lines. The Ga segregation at the surface is shown to produce a small shift in the energy positions of the Ga-3d states which is seen in UPS.[39] In this case, the spectra are in agreement with the data obtained from samples used in Ref. 41. Avoiding the Ga enrichment leads to a reduction of the Fermi level emission. These observations allow us to assume that the enhanced peak[40] at E_F is not, at least to some extent, an intrinsic property of $PuCoGa_5$.

Comparison between the theory and PE experiments is often taken as an important criterion of truthfulness of the electronic structure calculations. The use of the single-particle LDA DOS to compare with the PE spectrum would assume weak electron correlations among the 5f states in $PuCoGa_5$. For 5f states at the borderline between the localized and itinerant behavior neither LDA nor static-mean-field LDA+U theories are sufficient to accurately describe the photoemission,[41] since these approximations entirely miss the experimentally observed atomic-like multiplets.

The LDMA has been demonstrated to be capable of describing the multiplet transitions in elementary actinides rather well.[8] In Fig. 3 we show the total and f-projected spectral density for the Pu atom in $PuCoGa_5$ as provided by LDMA calculations. The f states are mostly concentrated in the binding energy range 0.5–2 eV with additional small satellites found at around 3 eV. Their positions are overlapping with the Co-d states located in the range 0.5–2.5 eV. No significant peak in the f-projected spectral density is found in the vicinity of the Fermi level, only a small contribution from the f states remains at E_F. Overall, our calculations are in fair agreement with experimental PE spectra.[39]

IV. CONCLUSIONS

Our correlated band theory calculations show that the LDA picture of the electronic structure dominated near the Fermi level by delocalized 5f electrons is modified when the electron correlations are taken into account more accurately. Both the LDA+U and LDMA calculations indicate that the plutonium f shell is different from the f^5 configuration. We obtain the f-shell occupation $n_f \approx 5.3$ implying an intermediate-valence state of Pu in $PuCoGa_5$ and $PuRhGa_5$ compounds. An explicit account for the Coulomb repulsion in the 5f shell leads to a reduction of the f character of the electronic states at the Fermi level compared to LDA, and gives an indication of a substantial hybridization between f and non-f states. It is shown that correlated band theory reproduces the correct nonmagnetic ground state and provides a good description of electric-field gradients and valence-band photoemission spectra for $PuCoGa_5$ and $PuRhGa_5$ compounds. The calculated electronic spectrum displays a pseudogap that could be related to the hybridization gap observed in recent experiments.[28] Our findings can be important for understanding the superconductivity in these materials.

ACKNOWLEDGMENTS

We acknowledge stimulating discussions with R. Caciuffo, G.H. Lander, and T. Durakiewicz and financial support from Czech Republic Grants No. GACR P204/10/0330, GAAV IAA100100912, and AV0Z10100520, and from the Swedish Research Council, STINT and SNIC. J.K. acknowledges support by the Alexander von Humboldt foundation.

[1] J. L. Sarrao, L. A. Morales, J. D. Tompson, B. L. Scott, G. R. Stewart, F. Wastin, J. Rebizant, P. Boulet, E. Colineau, and G. H. Lander, Nature (London) **420**, 297 (2002).

[2] N. J. Curro, T. Caldwell, E. D. Bauer, L. A. Morales, M. J. Graf, Y. Bang, A. V. Balatsky, J. D. Thompson, and J. L. Sarrao, Nature (London) **434**, 622 (2005).

[3]A. Hiess, A. Stunault, E. Colineau, J. Rebizant, F. Wastin, R. Caciuffo, and G. H. Lander, Phys. Rev. Lett. **100**, 076403 (2008).
[4]I. Opahle and P. M. Oppeneer, Phys. Rev. Lett. **90**, 157001 (2003).
[5]A. B. Shick, V. Janiš, and P. M. Oppeneer, Phys. Rev. Lett. **94**, 016401 (2005).
[6]P. M. Oppeneer, S. Elgazzar, A. B. Shick, I. Opahle, J. Rusz, and R. Hayn, J. Magn. Magn. Mater. **310**, 1684 (2007).
[7]L. V. Pourovskii, M. I. Katsnelson, and A. I. Lichtenstein, Phys. Rev. B **73**, 060506 (2006).
[8]A. B. Shick, J. Kolorenč, A. I. Lichtenstein, and L. Havela, Phys. Rev. B **80**, 085106 (2009).
[9]A. B. Shick, J. Kolorenč, A. I. Lichtenstein, and L. Havela, IOP Conf. Series: MSE **9**, 012049 (2010).
[10]E. Wimmer, H. Krakauer, M. Weinert, and A. J. Freeman, Phys. Rev. B **24**, 864 (1981).
[11]A. B. Shick, A. I. Liechtenstein, and W. E. Pickett, Phys. Rev. B **60**, 10763 (1999); A. B. Shick and W. E. Pickett, Phys. Rev. Lett. **86**, 300 (2001).
[12]P. Blaha, K. Schwarz, G. K. H. Madsen, D. Kvasnicka, and J. Luitz, WIEN2k, Vienna University of Technology, 2001 (ISBN 3-9501031-1-2).
[13]P. Blaha, K. Schwarz, and P. Herzig, Phys. Rev. Lett. **54**, 1192 (1985).
[14]P. Herzig, Theor. Chim. Acta **67**, 323 (1985).
[15]P. Mohn, Hyperfine Int. **128**, 67 (2000).
[16]To simplify the notation, we show the Pauli-like Hamiltonian including spin-orbit coupling, while the actual implementation contains also the scalar-relativistic terms.
[17]M. T. Czyzyk and G. A. Sawatzky, Phys. Rev. B **49**, 14211 (1994).
[18]J. C. Lashley, A. C. Lawson, R. J. McQueeney, and G. H. Lander, Phys. Rev. B **72**, 054416 (2005).
[19]J. Rusz, P. M. Oppeneer, N. J. Curro, R. R. Urbano, B.-L. Young, S. Lebègue, P. G. Pagliuso, L. D. Pham, E. D. Bauer, J. L. Sarrao, and Z. Fisk, Phys. Rev. B **77**, 245124 (2008).
[20]N. J. Curro, T. Caldwell, E. D. Bauer, L. A. Morales, M. J. Graf, Y. Bang, A. V. Balatsky, J. D. Thompson, and J. L. Sarrao, Physica B **378–380**, 915 (2006).
[21]N. Curro, private communication. In our understanding, the fit to the measured quadrupolar resonances in Ref. 20 most likely converged to a local minimum, where the local symmetries of Ga(1) and Ga(2) sites got interchanged. The value of 28.28 MHz assigned to Ga(1) actually covers the span of observed frequencies, while η and 8.14 MHz are best fits for the remaining variance of the data, but their physical significance is not evident. Therefore the fitted 28.28 MHz NQR frequency can at the best be considered as an approximation of the Ga(2) quadrupolar frequency.
[22]H. Sakai, Y. Tokunaga, T. Fujimoto, S. Kambe, R. E. Walstedt, H. Yasuoka, D. Aoki, Y. Homma, E. Yamamoto, A. Nakamura, Y. Shiokawa, K. Nakajima, Y. Arai, T. D. Matsuda, Y. Haga, and Y. Onuki, J. Phys. Soc. Jpn. **74**, 1710 (2005).
[23]D. Lide, *CRC Handbook of Chemistry and Physics* (CRC Press, Taylor & Francis LLC, Boca Raton, 2004).
[24]K. T. Moore and G. van der Laan, Rev. Mod. Phys. **81**, 235 (2009).
[25]J. H. Shim, K. Haule, and G. Kotliar, Europhys. Lett. **85**, 17007 (2009).
[26]R. Settai, H. Shishido, S. Ikeda, Y. Murakawa, M. Nakashima, D. Aoki, Y. Haga, H. Harima, and Y. Onuki, J. Phys. Condens. Matter **13**, L627 (2001).
[27]A. C. Hewson, *The Kondo Problem to Heavy Fermions* (Cambridge University Press, Cambridge, 1993).
[28]D. Talbayev, K. S. Burch Elbert, E. M. Chia, S. A. Trugman, J.-X. Zhu, E. D. Bauer, J. A. Kennison, J. N. Mitchell, J. D. Thompson, J. L. Sarrao, and A. J. Taylor, Phys. Rev. Lett. **104**, 227002 (2010).
[29]P. B. Allen, Phys. Rev. B **36**, 2920 (1987).
[30]P. Piekarz, K. Parlinski, P. T. Jochym, A. M. Oleś, J. P. Sanchez, and J. Rebizant, Phys. Rev. B **72**, 014521 (2005).
[31]S. Raymond, P. Piekarz, J. P. Sanchez, J. Serrano, M. Krisch, B. Janoušová, J. Rebizant, N. Metoki, K. Kaneko, P. T. Jochym, A. M. Oleś, and K. Parlinski, Phys. Rev. Lett. **96**, 237003 (2006).
[32]F. Jutier, G. A. Ummarino, J.-C. Griveau, F. Wastin, E. Colineau, J. Rebizant, N. Magnani, and R. Caciuffo, Phys. Rev. B **77**, 024521 (2008).
[33]W. L. McMillan, Phys. Rev. **167**, 331 (1968).
[34]G. A. Ummarino, N. Magnani, J. C. Griveau, J. Rebizant, and R. Caciuffo, J. Nucl. Mater. **385**, 4 (2009).
[35]I. Schnell, I. I. Mazin, and A. Y. Liu, Phys. Rev. B **74**, 184503 (2006).
[36]M. L. Kulić, Phys. Rep. **338**, 1 (2000).
[37]P. Javorský, E. Colineau, F. Wastin, F. Jutier, J.-C. Griveau, P. Boulet, R. Jardin, and J. Rebizant, Phys. Rev. B **75**, 184501 (2007).
[38]E. D. Bauer, T. Park, R. D. MacDonald, M. J. Graf, L. N. Boulaevskii, J. N. Mitchell, J. D. Thompson, and J. L. Sarrao, J. Alloy Comp. **488**, 554 (2009).
[39]R. Eloirdi, L. Havela, T. Gouder, A. B. Shick, J. Rebizant, F. Huber, and R. Caciuffo, J. Nucl. Mater. **385**, 8 (2009).
[40]J. J. Joyce, J. M. Wills, T. Durakiewicz, M. T. Butterfield, E. Guziewicz, J. L. Sarrao, L. A. Morales, A. J. Arko, and O. Eriksson, Phys. Rev. Lett. **91**, 176401 (2003).
[41]J. H. Shim, K. Haule, and G. Kotliar, Nature (London) **446**, 513 (2007).